Experimental Evaluation of an Analog Gain Optimization Algorithm in Optical Camera Communications

Vicente Matus, Victor Guerra, Cristo Jurado-Verdu, Shivani Rajendra Teli, Stanislav Zvanovec, Jose Rabadan, Rafael Perez-Jimenez

Experimental Evaluation of an Analog Gain Optimization Algorithm in Optical Camera Communications

Vicente Matus
IDeTIC-ULPGC,
Las Palmas de Gran Canaria, Spain
vmatus@idetic.eu

Victor Guerra
IDeTIC-ULPGC,
Las Palmas de Gran Canaria, Spain
vguerra@idetic.eu

Cristo Jurado-Verdu
IDeTIC-ULPGC,
Las Palmas de Gran Canaria, Spain
cjurado@idetic.eu

Shivani Rajendra Teli
Czech Technical University
Prague, Czech Republic
telishiv@fel.cvut.cz

Stanislav Zvanovec
Czech Technical University
Prague, Czech Republic
xzvanove@fel.cvut.cz

Jose Rabadan
IDeTIC-ULPGC,
Las Palmas de Gran Canaria, Spain
jrabadan@idetic.eu

Rafael Perez-Jimenez
IDeTIC-ULPGC,
Las Palmas de Gran Canaria, Spain
rperez@idetic.eu

***Abstract*—The operation of Optical Camera Communication systems in outdoor conditions is challenged by interfering sources of light and optical attenuation induced by the atmosphere. The low signal power at the receiver is prone to be affected by the quantization noise at the analog-to-digital converter. In this paper, an algorithm for optimizing the camera's analog gain has been experimentally evaluated under laboratory conditions. The image quality improvement is estimated by Pearson's correlation coefficient to a template signal, and it is shown to improve the signal-to-noise ratio up to 27.8 dB.**

***Index Terms*—Optical Camera Communications, analog gain, Pearson's correlation coefficient, signal-to-noise ratio.**

I. INTRODUCTION

Optical Camera Communication (OCC) is a group of schemes within the Visible Light Communication (VLC) field to be included in the IEEE 802.15.7r1 [1], and where the main principle is to use a digital camera as a receiver (R_x), taking advantage of the low price of these devices. In OCC, the extensive use of Rolling Shutter (RS) cameras is based on their ability to scan lines of pixels delayed between each other by orders of tens of μs [2]. These cameras are the most available in commercial devices using Complementary Metal-Oxide-Semiconductor (CMOS) sensors [3], [4]. The signal coming from a Light Emitting Diode (LED) transmitter (T_x) is captured by the lines of the sensor at different times, allowing the receivers to decode several symbols from each image frame.

Outdoor applications of OCC such as localization, Vehicular VLC, and Sensor Networks, face relevant challenges such as long link spans, optical degradation by atmospheric conditions [5], and require mobility support in most cases. Applications such as VLC positioning specifically rely on beacon signals, and most systems use packet structures with well-known patterns for the detection of Region of Interest (ROI) and synchronization. Correlators can be used for the recognition of such patterns [6].

The signal-to-noise ratio (SNR) at the receiver is crucial for allowing any communication link to have longer spans. The SNR depends on the transmitted power, on the attenuation factor of the channel, and in the case of OCC, it also depends on the optical lens array of the camera. In addition, an OCC system can be exposed to various sources of noise and interference. The area of the transmitter projected over the imaging sensor is also relevant in OCC, the maximum link distance is then bounded by the amount of sensor rows covered by the transmitter, in the case of RS-OCC. Geometrical derivations can estimate the image projected area [7]. The SNR can be estimated from the data-containing pixels

In this work, the use of an analog gain control algorithm for optimizing the SNR through a cost function based on the correlation is proposed. The correlation is extensively used for spatial synchronization and channel estimation in OCC. Therefore, the inclusion of this control algorithm will have little or no impact on computation performance of the R_x if the correlation is considered already a process of other algorithms. Several experiments involving different input powers, the algorithm's convergence iteration, and the SNR improvement are also provided.

The structure of this paper is the following. The OCC channel of an RS-based OCC system is modelled in II. The control algorithm for the optimization of the signal quality is derived in Section III. Both methodology and experimental design are described in Section IV. In Section V, the results obtained from the experiments are discussed. Finally, the conclusions of this work are drawn in Section VI.

This project has received funding from the European Union's Horizon 2020 research and innovation programme under the Marie Skłodowska-Curie grant agreement No 764461.

II. OCC Channel

The simplified diagram of an outdoor OCC scenario is shown in Fig. 1 in which a VLC transmitter using On-Off Keying (OOK) modulation sends pulses of each of the red-green-blue (RGB) colors. The shape of the ROI or the pixels of the frame that are exposed to the transmitted signal is not necessarily known beforehand. The attenuation of some atmospheric conditions that might be present, *e.g.* in foggy weather, is modeled by A in dB/m. The link span d in m depends on the relative position of the source with respect to the camera and its orientation, which in most cases are constantly changing.

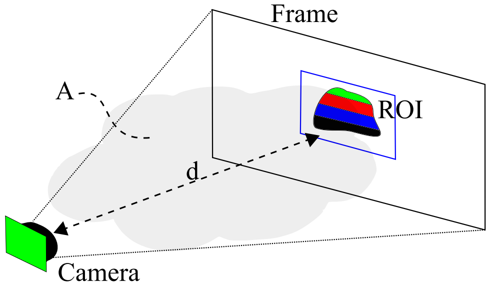

Fig. 1. Simplified diagram of the RS-OCC system considered.

The power signal at the receiver $P_{Rx}(t)$ under an attenuated channel, when the transmitter is modeled as an m-order Lambertian source with power $P_{Tx}(t)$, can be expressed as

$$P_{Rx}(t) = P_{Tx}(t)e^{-Ad} \cdot \frac{m+1}{2\pi} \cdot \cos^m \theta \frac{A_{lens} \cos \Psi}{d^2}, \quad (1)$$

where θ is the emission angle, Ψ is the incident angle, and A_{lens} is the area of the camera's external lens. From this expression, it can be seen that by varying either the transmitted power or the factor $A{\cdot}d$, known as the optical density, the received power can be affected alternatively, allowing to emulate the effect of the other parameters. Note that the projected area of the source over the camera sensor is mostly only dependent on d.

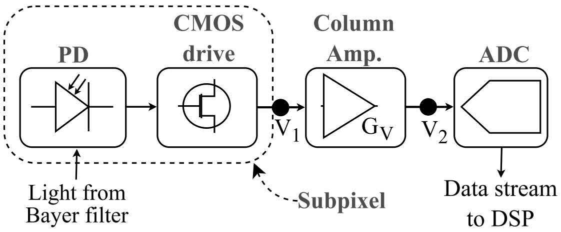

Fig. 2. Typical configuration of Complementary Metal-Oxide-Semiconductor (CMOS) camera sub-pixels.

In Fig. 2, the block diagram of a regular CMOS camera sub-pixel is shown, as described in [8]. The photodiode (PD) at position x, y and channel $c \in \{R, G, B\}$ receives light from a colored Bayer filter and generates a current $i_{pd}(x, y, c)$ which is turned into a voltage signal V_1 by the CMOS drive. Since the sequential reading by rows allows it, an analog amplifier and analog-to-digital converter (ADC) are shared by each column of sub-pixels of the sensor. The gain of the analog amplifiers G_V is set globally by the software of the camera and the voltage signal that is sampled by the ADC is given by $V_2 = G_V \cdot V_1$. The ADC induces a noise (σ^2_{adc}), that can be modeled as a random Normal of mean zero with a variance that depends on the digitalization levels. The SNR of the signal that enters the digital signal processing (DSP) block can be modeled as

$$SNR \approx \frac{G_V^2 \cdot i_{pd}^2(x,y,c)}{G_V^2\left(\sigma_{th}^2 + \sigma_{sh}^2\right) + \sigma_{adc}^2}, \quad (2)$$

where σ^2_{th} and σ^2_{sh} correspond to the thermal noise and shot noise of the process, respectively. Note that the noise induced by the ADC can be virtually reduced to zero by increasing G_V as

$$\lim_{G_V \to \infty} SNR = \frac{i_{pd}^2(x,y,c)}{\sigma_{th}^2 + \sigma_{sh}^2}, \quad (3)$$

nevertheless, the ADC has an upper bound for the input voltage, then G_V can only be increased up to the point V_2 does not saturate the ADC.

In previous work [9], it was shown that the SNR can be obtained empirically from image frames. Nevertheless, its computation can be substituted by the calculation of the Pearson's correlation coefficient r_{xy} between the image frames and a well known template, which is used in some implementations of OCC for synchronization of the received signal in the images and also for ROI detection. The parameter r_{xy} is defined as

$$r_{xy} = \frac{\sum_{i=1}^{N}(x_i - \bar{x})(y_i - \bar{y})}{\sqrt{\sum_{i=1}^{N}(x_i - \bar{x})^2}\sqrt{\sum_{i=1}^{N}(y_i - \bar{y})^2}}, \quad (4)$$

where x_i are the rows of the template of size N rows, y_i are N consecutive rows of the image, and $\bar{x}, \bar{y}$ are the mean values. The computation is iterated for all possible subsets $y_j, y_{j+1}, ..., y_{j+N-1}, (j + N - 1) < M$ of consecutive rows of the frame. When the template is matched in phase with the signal it emulates, the maximum value r_{xy}^{max} is achieved. This value is considered the overall correlation between the image frame and the template, which has been shown to be closely related to the SNR, giving high values of r_{xy}^{max} when the signal quality is high [9].

III. Analog Gain Control Algorithm

As it was aforementioned, r_{xy}^{max} is closely related to SNR, and may serve as a fast estimator of it. Therefore, optimizing the correlation using G_V would implicitly maximize SNR. The following paragraphs describe each one of the development of the algorithm for controlling G_V to maximize r_{xy}^{max} proposed in this work, which is based on the typical feedback-based design, as shown in Fig. 3.

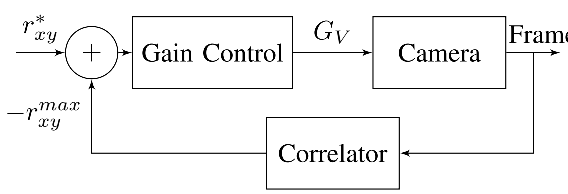

Fig. 3. Block diagram of the gain control algorithm.

The set point r^*_{xy} is the desired value for r^{max}_{xy} to be achieved by the controller, which is set to 1 in order to force the system to get the highest signal quality.

The camera block receives each updated value of G_V and sets this parameter on the physical device. Generally, camera's do not have a continuum of analog gains, but a discrete range of possible values. In this work, since Sony IMX219 image sensor is considered, the possible gains in linear units is defined by

$$G_V(X) = \frac{256}{256 - X}, \tag{5}$$

where X is an integer between 0 and 232 (233 possible analog gains). Due to the hyperbolic nature of $G_V(X)$, there is higher resolution at lower gain values. Furthermore, this quantization could be considered as an extra noise term, since each iteration will probably not coincide with valid values.

Finally, this block also captures the image and passes it to the correlation calculation block, which carries out Pearson's correlation coefficient with a parametric template. The maximum value of this operation is then forwarded to the gain control algorithm.

Mathematically, it is straightforward to define a cost function $C(G_V)$ that optimizes r^{max}_{xy} as

$$C(G_V) = \left(1 - r^{max}_{xy}\right)^2. \tag{6}$$

The performance of the control algorithm would significantly depend on the shape of the error curve. Nonetheless, in this work a simple squared difference scheme is proposed. $C(G_V)$ can be easily optimized using an iterative approach via a gradient descent on G_V, yielding

$$G_V^{(i+1)} = G_V^{(i)} - \lambda \frac{C\left(G_V^{(i)}\right)}{\partial C\left(G_V\right)/\partial G_V|_{G_V^{(i)}}}, \tag{7}$$

where λ is the learning rate or damping coefficient. It can be observed that the cost function's derivative can be reformulated as

$$\frac{\partial C(G_V)}{\partial G_V} = -2(1 - r^{max}_{xy})\frac{\partial r^{max}_{xy}}{\partial G_V}. \tag{8}$$

Since there is no closed-form relationship between r^{max}_{xy} and G_V, its derivative must be numerically estimated. In this work, a N-points linear regression was performed to obtain the curve's slope on the point of interest. However, the neighbourhood of the starting point must be explored during the algorithm's initialization by forcing a fixed analog gain change until an N-size estimation buffer is full to begin with the linear regressions, where N = 4 has been chosen arbitrarily.

Finally, combining equations (7) and (8), it yields the final iterative scheme, expressed as

$$G_V^{(i+1)} = G_V^{(i)} + \frac{\lambda}{2}\frac{1 - r^{max(i)}_{xy}}{\partial r^{max}_{xy}/\partial G_V|_{G_V^{(i)}}}. \tag{9}$$

The performance of the proposed algorithm would highly depend on the estimation of r^{max}_{xy}'s slope. As it was commented, this magnitude will be calculated using a linear regression of N points. Hence, the accuracy of the denominator in Equation (9) depends on the curve's shape, which will not be linear *a priori*, and the separation between samples.

IV. METHODOLOGY

It has been shown that the Pearson's correlation coefficient is a computationally quick estimator of the signal quality. Moreover, the camera analog gain can optimize the SNR by reducing quantization noise. The objective of this work is to propose a control algorithm for G_V based on the r_{xy} values obtained from each image capture. In order to demonstrate this hypothesis, a series of experiments were carried out using the experimental setup shown in Fig. 4. The scenario comprises a commercial RGB lamp controlled by a general purpose microcontroller [10] and a receiver built using an Element14 Raspberry Pi board with a camera based on Sony IMX sensor [11]. The lamp transmits pulses of a period T_{chip} and consecutively repeats a sequence of G-R-B-K pulses, where K stands for black, meaning it is an off state of the lamp. Different conditions can be emulated varying the LED power source voltage and using a Methacrylate sheet in order to emulate channel loss (optical density). The T_x and R_x parameters can be observed in Table I.

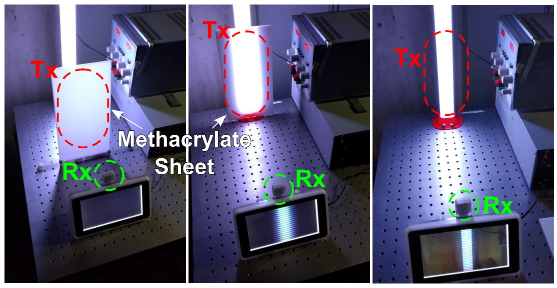

(a) (b) (c)

Fig. 4. Pictures of the experimental setup. In the experiments, the radiant energy at the camera position is 3.39 μW/cm^2 in (a) , 11.79 μW/cm^2 in (b), and 45.11 μW/cm^2 in (c)

TABLE I
Experiment key parameters.

Parameter	Value
	Transmitter
Device	12 V DC RGB LED strips
Front-end device	Atmel ATMega328p controller [10]
Power levels [W]	min = 1.8, max = 4.8
Dominant wavelengths [nm]	630 (Red), 530 (Green), 475 (Blue)
T_{chip} [s]	1/3600
	Receiver
Camera	Picamera V2 module (Sony IMX219) [11]
Resolution	3280 $\times$ 2464 px
t_{exp} [μs]	300
Gain (G_V) [dB]	0, ..., 20.6 (233 values)

The algorithm presented in Section III was evaluated for the three synthetic scenarios using different initial gain values ($G_V^{(0)}$). Furthermore, the estimation of the correlation's slope was based on N = 4 samples. The analyzed performance metric of the algorithms was the convergence iteration, estimated using:

$$r_{th} = r^{max(\infty)}_{xy}\left(1 \pm \varepsilon\right), \tag{10}$$

where $r^{max(\infty)}_{xy}$ is the final value after convergence, and ε is the threshold's parameter (which was set 0.05 arbitrarily for all experiments). The parameter r_{th} is the final threshold value of the correlation.

V. Results and Discussion

The first step of experimentation consisted on the acquisition of frames at all the available G_V values, and under three conditions of received intensity of radiant energy (I), as it is shown in Table II. These conditions were implemented by varying transmitted power and the channel attenuation, which derived in three different values of I at the receiver position. In each of the three conditions, the camera acquired images using the 233 available G_V values, repeating 50 times the acquisition, resulting in 11,650 frames under the same radiant energy conditions. These frames were processed to get the Pearson's correlation coefficient with respect to a template signal equal to the transmitted pulses of OOK.

TABLE II
Experiments conditions.

	I [μW/cm^2]	Gains [dB]	No. of Captures
Experiment 1	3.39	0 - 20.6	50 per each G_V
Experiment 2	11.79	0 - 20.6	50 per each G_V
Experiment 3	45.11	0 - 20.6	50 per each G_V

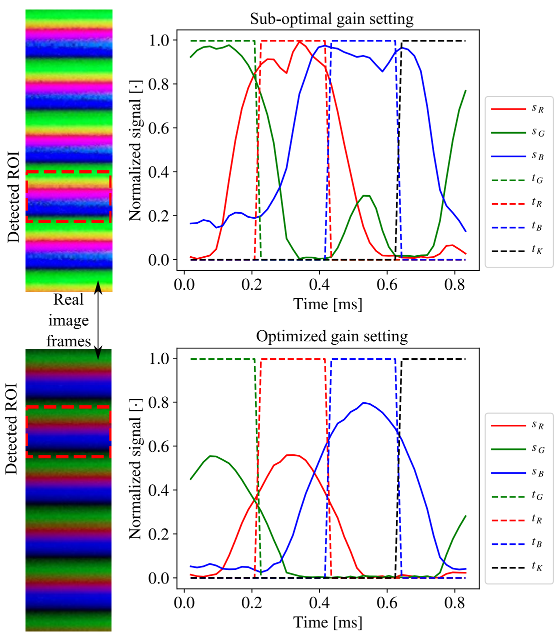

Fig. 5. Processing from two images obtained in the conditions of Experiment 3. The plot curves correspond to the R_x signal R-G-B channels, labeled as s_R, s_G, s_B, respectively, and the dashed curves to the template pulses G-R-B-K labeled as t_G, t_R, t_B, t_K, respectively. The picture insets represent a portion of the actual images captured. The red dashed line highlights the detected ROI.

In order to illustrate the impact of the variation of G_V in the image frames captured by the camera, Fig. 5 shows two signals obtained in the conditions of Experiment 3. The sub-optimal gain setting image was captured using G_V = 15.3 dB and the optimized gain setting image was captured using G_V = 2.0 dB. The images obtained r_{xy}^{max} = 0.76, and r_{xy}^{max} = 0.85, respectively, and the SNR obtained was 27.8 dB and 24.2 dB, respectively.

In Fig. 6, the average results of r_{xy}^{max} obtained from data acquisition and correlation processing are shown for the three experiments. The lowest received intensity of radiant energy at Experiment 1 shows more fluctuations of the correlation, and it shows that the contribution of G_V is to improve the signal quality since it is weak. In the other two experiments, a similar behaviour is seen. The high intensity of the received signal makes the gain to deteriorate the signal with saturation, which builds up mostly smoothly. In Experiments 2 and 3, the gain control algorithm should converge to the minimum gain values, and in Experiment 1, it should converge to the maximum gain. It is also important to note that none of the experiments have resulted in a r_{xy}^{max} curve with a maximum point at an intermediate value of G_V.

By setting arbitrary initial G_V values, the correlation data sets evaluated from Experiments 1, 2 and 3 were used to run the gain control algorithm for a fixed number of 150 iterations. In Fig. 7, the results of the chosen G_V at each iteration are shown. It can be seen that the Experiments 2 and 3 converge to the minimum gain, as expected, in which the correlation is the maximum. The convergence is obtained after about 25 iterations. For the case of Experiment 1, the algorithm takes longer to converge, after about 60 iterations.

The results obtained show that the gain control algorithm can successfully converge to the gain value that ensures maximum correlation available in each scenario. Considering a standard frame rate of 30 fps, and negligible delays at the DSP, the algorithm could converge in about 1 s.

VI. Conclusions

This work shows the development an algorithm for the automated control of analog gain in a CMOS sensor camera used in an experimental RS-based OCC under laboratory conditions that emulated an optical attenuation of the signal across the channel. It was shown that the camera analog amplifier stage before the ADC can reduce the quantization noise only if it does not saturate the ADC, thus, the optimal value of G_V can vary depending on the transmitted power and the attenuation induced by the channel. In addition, the use of Pearson's correlation coefficient was shown to be an estimator of the signal quality at the R_x, as an alternative to the calculation of SNR. The algorithm was developed for the use of r_{xy}^{max} as the feedback, allowing to estimate the next capture's G_V to maximize the quality. It was found that in high received power cases, the algorithm converges to the optimal gain in about 25 iterations, whereas in low received power cases, it takes more than double the amount of iterations. With these values, and considering a standard 30 fps frame rate of the camera, the convergence time is between 1 and 2 s. In case of mobility or changing conditions, it would be necessary to repeatedly run the algorithm. For future work, the parameters of the control algorithm such as damping coefficient and gain seed need to be optimized in more realistic conditions. It is also necessary to demonstrate its convergence under conditions where the optimal G_V is an intermediate value.

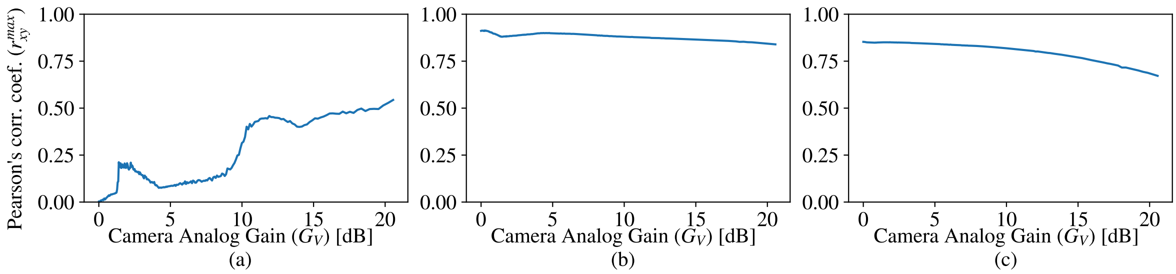

Fig. 6. Data acquisition average values of r_{xy}^{max} obtained varying G_V over all the available values. Results from Experiment 1 are shown in (a), Experiment 2 in (b), and Experiment 3 in (c).

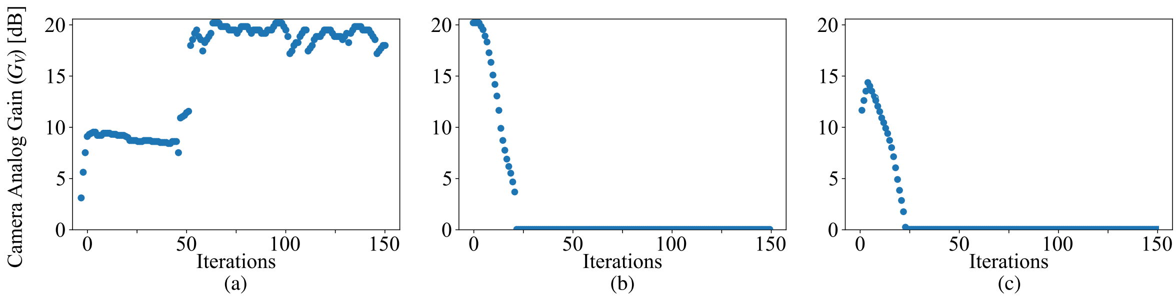

Fig. 7. Convergence of the algorithm in each of the experiments, where (a) corresponds to Experiment 1, (b) to Experiment 2, and (c) to Experiment 3.

References

[1] W. A. Cahyadi, Y. H. Kim, Y. H. Chung, and C. Ahn, "Mobile phone camera-based indoor visible light communications with rotation compensation," *IEEE Photonics Journal*, vol. 8, no. 2, pp. 1–8, April 2016.

[2] T. Nguyen, Chang Hyun Hong, Nam Tuan Le, and Y. M. Jang, "High-speed asynchronous optical camera communication using led and rolling shutter camera," in *2015 Seventh International Conference on Ubiquitous and Future Networks*, July 2015, pp. 214–219.

[3] R. Boubezari, H. Le Minh, Z. Ghassemlooy, and A. Bouridane, "Smartphone camera based visible light communication," *Journal of Lightwave Technology*, vol. 34, no. 17, pp. 4121–4127, Sep. 2016.

[4] T. Nguyen, A. Islam, T. Hossan, and Y. M. Jang, "Current status and performance analysis of optical camera communication technologies for 5g networks," *IEEE Access*, vol. 5, pp. 4574–4594, 2017.

[5] A. Islam, M. T. Hossan, and Y. M. Jang, "Convolutional neural networkscheme–based optical camera communication system for intelligent internet of vehicles," *International Journal of Distributed Sensor Networks*, vol. 14, no. 4, p. 1550147718770153, 2018.

[6] C. Jurado-Verdu, V. Matus, J. Rabadan, V. Guerra, and R. Perez-Jimenez, "Correlation-based receiver for optical camera communications," *Opt. Express*, vol. 27, no. 14, pp. 19 150–19 155, Jul 2019.

[7] P. Chavez-Burbano, V. Guerra, J. Rabadan, D. Rodríguez-Esparragón, and R. Perez-Jimenez, "Experimental characterization of close-emitter interference in an optical camera communication system," *Sensors*, vol. 17, no. 7, p. 1561, Jul 2017.

[8] T. Kuroda, *Essential Principles of Image Sensors*. CRC Press, 2017.

[9] V. Matus, E. Eso, S. R. Teli, R. Perez-Jimenez, and S. Zvanovec, "Experimentally derived feasibility of optical camera communications under turbulence and fog conditions," *Sensors*, vol. 20, no. 3, p. 757, Jan 2020.

[10] Atmel Corporation, *ATmega328p, 8-bit AVR Microcontroller with 32K Bytes In-System Programmable Flash, Datasheet*. Atmel Corporation, 2015.

[11] Sony Corporation, *IMX219PQH5-C, Diagonal 4.60 mm (Type 1/4.0) 8 Mega-Pixel CMOS Image Sensor with Square Pixel for Color Cameras, Datasheet*. Sony Corporation, 2014.